ELSEVIER

Agricultural and Forest Meteorology 68 (1994) 201–212

AGRICULTURAL AND FOREST METEOROLOGY

Modelling the effect of mean pressure gradient on the mean flow within forests

Xuhui Lee*[,a], Roger H. Shaw[b], T. Andrew Black[a]

[a]*Department of Soil Science, University of British Columbia, Vancouver, B.C. V6T 1Z4, Canada*

[b]*Department of Land, Air and Water Resources, University of California, Davis, CA 95616-8627, USA*

(Received 5 November 1992; revision accepted 6 September 1993)

Abstract

Air flow within forests was simulated using models based on first- and second-order closure principles, with the addition of the mean barometric pressure gradient in the momentum equation. The simulations indicate that the mean pressure gradient can have a strong influence on the mean wind speed profiles within forests. The inclusion of the pressure term can improve both models in terms of their capacities to match observations. The simulations also demonstrate that significant wind direction shear can occur within a forest.

1. Introduction

In a horizontally homogeneous vegetation stand under steady state conditions, the temporally averaged equation for momentum along the longitudinal direction can be written as

$$\frac{\partial \overline{-u'w'}}{\partial z} = \frac{1}{\rho}\frac{\partial P}{\partial x} + C_d a \bar{u} |\vec{U}| \tag{1}$$

where the term on the left-hand side of Eq. (1) is the vertical divergence of the longitudinal kinematic Reynolds stress ($\overline{-u'w'}$), the first term on the right-hand side is the mean longitudinal kinematic pressure gradient, and the second term is the drag imposed on the mean flow by plant elements, with C_d being the drag coefficient, a the element area density, $\bar{u}$ the longitudinal velocity component, and $\vec{U}$ the horizontal

* Corresponding author.

SSDI 0168-1923(93)02118-P

Table 1
A list of the inputs to the models: height of the stand (h), total (leaf + stem) element area density (L), longitudinal velocity ($\bar{u}$) and friction velocity (u_*) at $z = h$, and drag coefficient (C_d)

Stand	h (m)	L	$\bar{u}(h)$ ($m\,s^{-1}$)	u_* ($m\,s^{-1}$)	C_d	Source
Corn crop	2.8	3.0	2.09	0.60	0.20	Shaw et al. (1974), Shaw (1977)
Deciduous forest	23.0	5.5	0.90	0.42	0.15	Baldocchi and Meyers (1988a,b)
Coniferous forest	16.7	5.7	1.95	0.39	0.15	Lee and Black (1993)

velocity vector. The Coriolis force and molecular transport are at least one order of magnitude smaller than the terms in Eq. (1) and are excluded from the discussion. In short agricultural crops, the pressure term is much smaller than the Reynolds stress divergence term, as shown by Finnigan (1979), and can be neglected in Eq. (1). In a forest, where the Reynolds stress divergence and canopy drag are small owing to the tallness of the stand and the sparseness of the plant elements, respectively, the pressure term can be significant. This is definitely so in the open trunk space. For example, $\partial P/\partial x$ has a typical magnitude of 1 hPa (100 km)$^{-1}$ or 8.3×10^{-4} m s^{-2} for $(1/\rho)\partial P/\partial x$ for synoptic weather systems at middle latitudes (e.g. Wallace and Hobbs, 1977), and $C_d a \bar{u}|\vec{U}|$ is estimated to be 4.5×10^{-4} m s^{-2}, with $C_d = 0.15$ (see Table 1), $|u| = |\vec{U}| = 0.5$ m s^{-1}, and $a = 0.012$ m^{-1} (a value corresponding to a tree density of 600 stems ha^{-1} and an average trunk diameter of 0.2 m). The two terms are of similar magnitude.

Holland (1989) hypothesized that in the lower portions of a deep forest the mean wind speed and fluctuations of wind velocity result primarily from the mean horizontal pressure gradient and local fluctuations of the pressure gradient, respectively. Experimental studies have suggested that pressure fluctuations are, to a large extent, responsible for many turbulent aspects of subcrown air movement (Shaw et al., 1990; Shaw and Zhang, 1992). There is also evidence of interactions between the mean pressure gradient and the mean flow in forests, e.g. the change of wind direction with height (Shinn, 1971; Smith et al., 1972; Pinker and Holland, 1988) and upward momentum flux (Lee and Black, 1993) within the stand.

Over the past three decades, a number of models have been developed for flow through vegetation canopies, based on mixing-length (gradient-diffusion) theory (Cionco, 1965; Smith et al., 1972; Li et al., 1985, 1990), the K-ϵ method (Green, 1993), higher order closure principles (Wilson and Shaw, 1977; Meyers and Paw U, 1986; Wilson 1988) and large eddy simulations (Shaw and Schumann, 1992). A few of these modelling studies have taken the pressure gradient effect into account. In attempts to explain the turning of the wind with height in forests, Smith et al. (1972) and Shinn (1971) simplified the flow field to a balance between the Reynolds stress gradient and either form drag in the canopy layer or pressure gradient in the trunk space. They used a constant mixing length to relate mean wind speed to Reynolds stress and solved the flow equations analytically. Kondo and Akashi

(1976) advanced their analyses to allow the mixing length and plant area density to change with height and solved the equations numerically. In their model the surface pressure gradient was expressed in terms of the geostrophic wind. Since their focus was the effect of the vertical plant area density distribution on the flow within canopies, a single value was assigned to the geostrophic wind for all their calculations. In cases where local perturbations exist, however, the surface pressure gradient cannot be directly related to the geostrophic wind. Later, Yamada (1982) included the pressure term in modelling flow within a horizontally homogeneous forest, but he did not show sufficient detail to resolve the wind profile within the stand. The pressure term was also included in the model of Li et al. (1990) for flow through forest edges, but the term was confined to the perturbed pressure field and the ambient one was ignored.

The purpose of this paper is to test the effect of the surface pressure gradient on the flow within extensive horizontally homogeneous canopies under steady state conditions. Two models will be used: a first-order closure (FOC) model using the mixing length parameterization and a second-order closure (SOC) model based on the principles established by Wilson and Shaw (1977). Both models are formulated in two-dimensional forms and represent two levels of complexity. Unlike the study of Kondo and Akashi (1976), the surface pressure gradient terms are expressed explicitly in the flow equations so that its effect can be examined by directly assigning different values to these terms. The models are applied to flow in three stands, a coniferous forest (Lee and Black, 1993), a deciduous forest (Baldocchi and Meyers, 1988a) and a corn crop (Shaw et al., 1974), and the numerical results are compared with observations.

2. The models

2.1. First-order closure

The FOC consists of Eq. (1), the momentum equation for the longitudinal direction, and that for the lateral direction as

$$\frac{\partial \overline{-v'w'}}{\partial z} = \frac{1}{\rho}\frac{\partial P}{\partial y} + C_d a \bar{v} |\vec{U}| \tag{2}$$

where $\overline{-v'w'}$ is the lateral kinematic Reynolds stress, $\bar{v}$ the lateral velocity component, and $(1/\rho)\partial P/\partial y$ the lateral kinematic pressure gradient.

The mixing length model is used to relate the Reynolds stress to the wind speed gradient such that

$$\overline{-u'w'} = l^2 \left|\frac{\partial \vec{U}}{\partial z}\right| \frac{\partial \bar{u}}{\partial z} \tag{3}$$

and

$$\overline{-v'w'} = l^2 \left|\frac{\partial \vec{U}}{\partial z}\right| \frac{\partial \bar{v}}{\partial z} \tag{4}$$

where l is the mixing length. The parameterization of Li et al. (1985) for l is adopted here as

$$l = \begin{cases} kz/(1.5 + 2.5a) & z \geq h_{max} \\ l_{hmax} + 0.3(z - h_{max}) & z < h_{max} \end{cases} \tag{5}$$

where h_{max} is the height of the maximum element area density and l_{hmax} is the mixing length at this height and is determined from Eq. (5) for $z > h_{max}$.

2.2. Second-order closure

The SOC scheme of Wilson and Shaw (1977) was originally formulated in the one-dimensional form and is extended here to two-dimensions. The basic equations include the momentum equations (Eqs. (1) and (2)), and the following equations:

Budget of Reynolds stress:

$$0 = -\overline{w'^2}\frac{\partial \bar{u}}{\partial z} + 2\frac{\partial}{\partial z}\left[q\lambda_1 \frac{\partial \overline{u'w'}}{\partial z}\right] - \frac{q}{3\lambda_2}\overline{u'w'} + Cq^2\frac{\partial \bar{u}}{\partial z} \tag{6}$$

$$0 = -\overline{w'^2}\frac{\partial \bar{v}}{\partial z} + 2\frac{\partial}{\partial z}\left[q\lambda_1 \frac{\partial \overline{v'w'}}{\partial z}\right] - \frac{q}{3\lambda_2}\overline{v'w'} + Cq^2\frac{\partial \bar{v}}{\partial z} \tag{7}$$

Budget of turbulent kinetic energy:

$$0 = -2\overline{u'w'}\frac{\partial \bar{u}}{\partial z} - 2\overline{v'w'}\frac{\partial \bar{v}}{\partial z} + \frac{\partial}{\partial z}\left[q\lambda_1 \frac{\partial q^2}{\partial z}\right] + 2\frac{\partial}{\partial z}\left[q\lambda_1 \frac{\partial \overline{w'^2}}{\partial z}\right] + 2C_d a|\vec{U}|^3 - 2\frac{q^3}{\lambda_3} \tag{8}$$

Budget of vertical velocity variance:

$$0 = 3\frac{\partial}{\partial z}\left[q\lambda_1 \frac{\partial \overline{w'^2}}{\partial z}\right] - \frac{q}{3\lambda_2}\left[\overline{w'^2} - \frac{q^2}{3}\right] - \frac{2}{3}\frac{q^3}{\lambda_3} \tag{9}$$

where $q = (\overline{u'^2} + \overline{v'^2} + \overline{w'^2})^{1/2}$, C is a constant, and λ_1, λ_2 and λ_3 are length scales that are proportional to a mixing length and related to the element area density (Wilson and Shaw, 1977).

2.3. Numerical methods

The boundary conditions used for the FOC model are $\bar{u} = \bar{u}(h)$ and $\bar{v} = 0$ at $z = h$ and $\bar{u} = \bar{v} = 0$ at $z = 0$. The substitution of Eqs. (3) and (4) into Eqs. (1) and (2) results in two nonlinear second-order differential equations for $\bar{u}$ and $\bar{v}$. The domain between $z = 0$ and $z = h$ is divided into 100 equally spaced intervals. The derivatives are approximated by the corresponding central differences at each grid point. Initial profiles are assumed and the solution is found iteratively. On a desk-top computer with an 80486 processor, the typical run time is about 5 s (40 iterations).

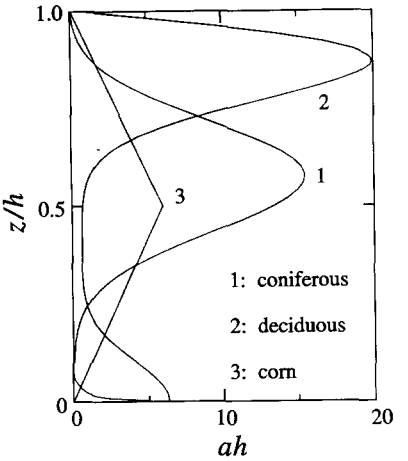

Fig. 1. Profiles of nondimensionalized element area density distribution, ah, for the three selected stands.

Smooth curves were fitted to the measured element area density distributions for the three selected stands (Fig. 1). For the corn crop, the area density distribution was approximated by a simple triangular distribution as in Shaw and Pereira (1982). Table 1 summarizes the relevant information regarding the three experiments. The value of C_d for the corn canopy is that of Wilson and Shaw (1977), and the value for the forests is similar to those of Li et al. (1985) and was determined so that the calculated values of $\bar{u}(h)/u_*$ were close to the measurements.

The boundary conditions for the SOC model include the conditions used by Wilson and Shaw (1977) and those for the lateral velocity and Reynolds stress. Specifically they are: (1) $\overline{u'w'} = -\bar{u}_{*2}^2, \bar{v} = 0, q^2 = 6.5u_{*2}^2$ and $\overline{w'^2} = 1.5u_{*2}^2$ at $z = 2h$, and (2) $\overline{u'w'} = -[k\bar{u}(Z)/\ln(Z/z_{so})]^2, \overline{v'w'} = -[k\bar{v}(Z)/\ln(Z/z_{so})]^2, q^2 = -6.5\overline{u'w'}, \overline{w'^2} = -1.5\overline{u'w'}$, and $\bar{u} = \bar{v} = 0$ at $z = 0$, where k (= 0.4) is the von Karman constant, $Z = 0.05h$, z_{so} (= $0.001h$) is the soil roughness length, and u_{*2} is the friction velocity (=$(-\overline{u'w'})^{0.5}$) at $z = 2h$. u_{*2} is determined, using Eq. (1), from the values of the friction velocity at $z = h$ (Table 1) and the longitudinal pressure gradient specified in each calculation. The domain between $z = 0$ and $z = 2h$ is divided into 200 equal grid spaces instead of the original 40 of Wilson and Shaw (1977). Such small grid spaces are needed in order to resolve the plant area near the floor of the coniferous forest (Fig. 1). To maintain consistency with Wilson and Shaw (1977), however, the components of Reynolds stress at the lower boundary are still evaluated from the velocities at 0.05 of the stand height. The solution is also found iteratively in a similar manner to that of the FOC model. The typical run time on the desk-top computer is about 10 min (170 iterations).

In the following sections, results are presented of the calculations using a single value of 135° for the angle between the surface pressure gradient and the longitudinal direction (θ_p). Additional calculations indicate that the profiles of the vector wind speed and Reynolds stress are insensitive to this angle.

3. Results and discussion

3.1. Wind speed

Figure 2(a) presents the profiles of the magnitude of the velocity vector calculated with the FOC model for the three stands. Several features are evident. The addition of the pressure gradient in the momentum equation, with a magnitude as small as 1 hPa $(100\ km)^{-1}$, a value typical for anticyclonic synoptic systems, results in secondary wind speed maxima. Such maxima are more pronounced in the forests than in the corn stand. The height of the simulated secondary maximum agrees well with the observations and is structure-dependent: the secondary maximum occurs at a higher relative level in the deciduous forest, where the overstory is distributed in a very thin layer near the top of the stand (Fig. 1), than in the coniferous forest, where the overstory is spread over a rather thick layer. Using a geostrophic wind of 7.5 m s^{-1} or a surface pressure gradient of 1 hPa $(100\ km)^{-1}$ and including the Coriolis force in their flow equations, Kondo and Akashi (1972) showed that the secondary maximum could occur in a stand with a relatively dense foliage layer and an open space near the ground, and that the maximum became more pronounced as the foliage density increased. On the other hand, our results indicate that the magnitude of the pressure gradient can be responsible for the existence and the magnitude of the maximum. Previously, Lee and Black (1993) reported that the mean wind speed at the height of the secondary maximum in the coniferous forest was least coupled with that above the

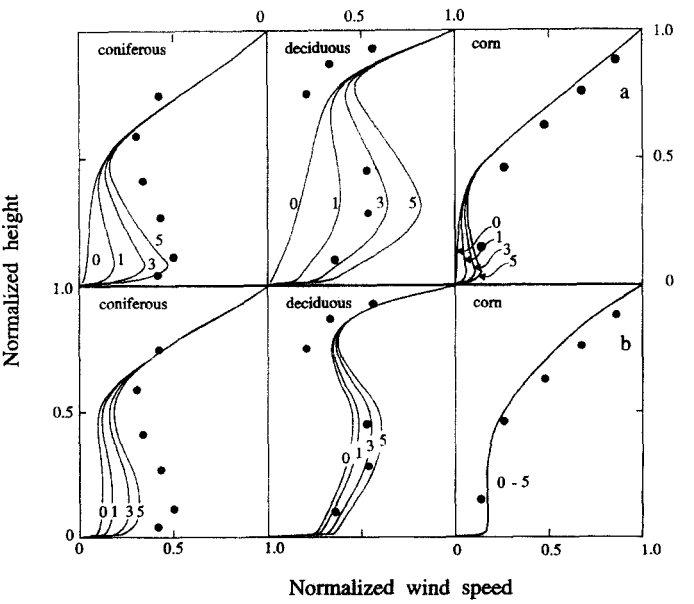

Fig. 2. Normalized vector wind speed profiles calculated with the first (a) and the second-order closure model (b). The numbers are the magnitudes of the surface pressure gradient (hPa $(100\ km)^{-1}$) and the dots indicate measurements.

stand, as compared with that at all other heights. It is possible that this could be viewed as the effect of the pressure gradient varying among the observation periods. Results of additional calculations with the inclusion of the Coriolis force in Eqs. (1) and (2) show no appreciable difference from those presented in Fig. 2.

Relatively high magnitudes of the surface pressure gradient are needed in order to produce strong secondary maxima comparable with the measurements within the two forests. Such magnitudes were possible during the experiments. As described by Lee and Black (1993), the coniferous forest was under the influence of strong thermally driven upslope/sea breezes. The associated surface pressure gradient, estimated from the divergence of the Reynolds stress above the stand, was in the order of 4–5 hPa $(100\ \text{km})^{-1}$. The wind at the deciduous site, on the other hand, was mainly a topographically modified one, primarily caused by the channeling of the synoptic-scale flow by the local terrain (Eckman et al., 1992). The topographic effect was interpreted as one of the reasons for the lack of constant Reynolds stress above the stand (Baldocchi and Meyers, 1988a). Based on the information on the local topography (Verma et al., 1986) and the theory proposed by Jackson and Hunt (1975) for flow over hills, the pressure gradient owing to the perturbation of the topography was estimated to be 2–3 hPa $(100\ \text{km})^{-1}$. The refinement of the model, however, requires precise determination of the surface pressure field in addition to measurements of turbulence within the stand and the stand structure. To our knowledge such experiments have yet to be reported in the literature.

Figure 2(b) presents the wind speeds calculated with the SOC model. Because Reynolds stress transport (term 2 in Eqs. (6) and (7)) is included in the flow equations, this model can produce weak to moderate secondary wind speed maxima within vegetation stands with zero pressure gradient. As with the FOC model, the calculations have been improved for the lower part of the two forest stands by the addition of the pressure gradient terms. Overall this model is less sensitive to the pressure gradient than the FOC model. This is especially so in the corn stand, where the pressure gradient effect can hardly be seen.

The mean absolute error of the normalized wind speed estimates of the FOC model, with the above probable magnitudes of the pressure gradient, is 0.10 for the coniferous forest and 0.16 for the deciduous forest. The corresponding values for the SOC model are 0.12 and 0.07. These errors are slightly higher than that reported by Meyers and Paw U (1986) (0.08, averaged for six stands). The SOC model tends to underestimate the wind speed in the lower part of the coniferous stand. There are several ways of improving the result of the SOC model. The constants of the model were originally evaluated against the observations in the corn stand. They may need to be adjusted according to the results of recent forest turbulence experiments. The transport of Reynolds stress is parameterized with the gradient diffusion method. A certain degree of smoothing is applied to the gradients of Reynolds stress in order to avoid a zero value of the transport term above the canopy and to make the transport non-local. This can be improved by using budget equations of third order moments (Meyers and Paw U, 1986).

Using the pressure gradient derived from the Reynolds divergence above the stand, the sensitivity of the normalized wind speed at the secondary maximum height within

the coniferous forest was estimated to be about 0.03 hPa $(100\ km)^{-1}$, similar to that of the SOC (0.04, Fig. 2(b)), but much smaller than that of the FOC (0.17, Fig. 2(a)). The high sensitivity of the wind profile computed using the FOC is almost certainly symptomatic of the manner in which the Reynolds stresses are parameterized (Eqs. (3) and (4)). Because the stresses are directly linked to the wind profiles, the inclusion of a pressure gradient in the FOC or a change in its magnitude must result in a change in the curvature of the wind profile. The wind velocity itself is obtained as a double integral of this curvature and can thus change substantially with the pressure field. On the other hand, the SOC schemes involve balance equations for the Reynolds stresses (Eqs. (6) and (7)) which include turbulent diffusion terms that allow non-local transport of momentum. Thus, the stresses are not immediately coupled with the local gradient of wind speed. As will be seen later (Fig. 5), the transport term assumes great importance in the Reynolds stress budget, illustrating that turbulence in the canopy is not a consequence only of local processes. The inability of FOC to deal with non-local effects must be considered a deficiency of this type of model.

3.2. Wind Direction Shear

In the case when the vertical Reynolds stress divergence is small in the lower part of a vegetation community, the drag force is mainly balanced by the pressure gradient force (Eqs. (1) and (2)). As a result, wind direction near the ground tends to align with $180° - \theta_p$ and significant wind direction shear can occur within the stand. This feature was observed in a gum-maple forest (Shinn, 1971) and is suggested by the simulations with the FOC model for the three stands with various surface pressure gradients (Fig. 3(a)). Unlike those of the FOC, the results of the SOC model indicate that little wind direction shear exists in the corn stand and that only under the influence of strong pressure gradients can wind direction near the floor of the two forests approach $180° - \theta_p$, i.e. 45° (Fig. 3(b)). Once again, the high sensitivity of the FOC model appears to be unrealistic because there is no evidence that there is a 45° turning of wind from the top to the bottom of corn canopies.

Wind direction shear was also simulated by Kondo and Akashi (1972) for canopies with various structures. They showed that the shear was more significant in denser stands. By comparing Fig. 3 with their results, it appears that the profile of wind direction is more sensitive to plant area density than to the surface pressure gradient.

3.3. Reynolds Stress

Compared with the wind field, the calculated Reynolds stress profile is less sensitive to the pressure gradient, particularly in the upper part of the stands. As an example, Fig. 4 shows the profiles for the coniferous forest after a coordinate rotation has been made following the procedure of Baldocchi and Hutchison (1987). This apparent insensitivity is a consequence of the fact that the pressure gradient significantly influences the wind speed only in the lower half of the forests (Fig. 2) where the Reynolds stress is small. The influence may be large in a relative sense but because the stresses have small magnitudes, there is little absolute change. With the addition

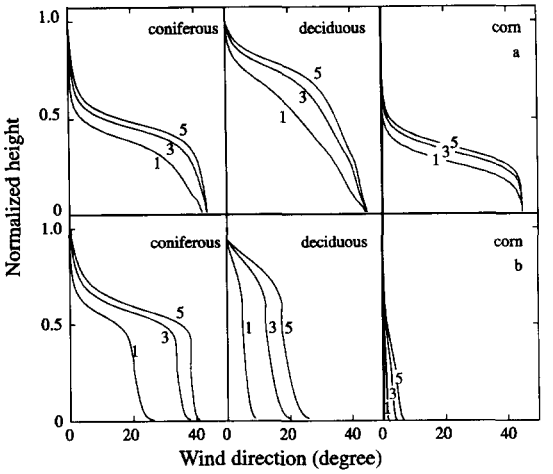

Fig. 3. Same as in Fig. 2 except for wind direction shear. The angle between the surface pressure gradient and the longitudinal direction (θ_p) is set at 135° . Wind direction is referenced to the longitudinal direction.

of a relatively large pressure gradient, both models produce slightly negative Reynolds stress, or upward momentum flux in the trunk space, but the magnitude is smaller than the observed one. This difference may be because the choice of the length scales is not accurate in the trunk space in both models.

Figure 5 shows the longitudinal Reynolds stress budget for the deciduous forest: shear production (term 1 of Eq. (6)), transport (term 2) and pressure velocity correlation or loss (the sum of terms 3 and 4). The addition of the pressure gradient does not alter the basic pattern, but increases the magnitudes of the normalized budget terms mainly by reducing u_{*2}. In the upper part of the crown layer and

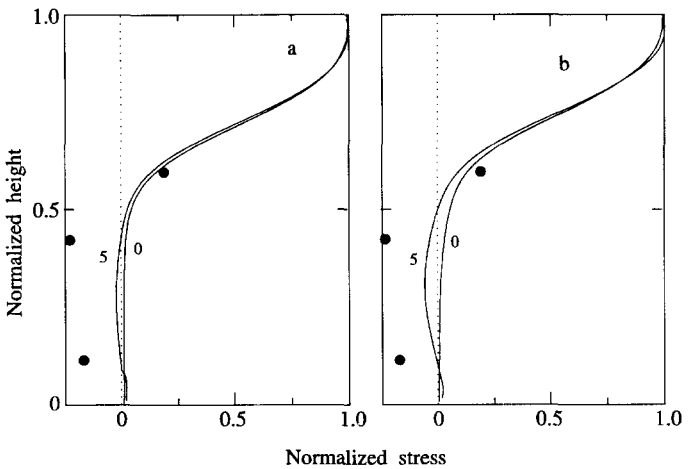

Fig. 4. Same as in Fig. 2 except for the normalized Reynolds stress profiles within the coniferous forest.

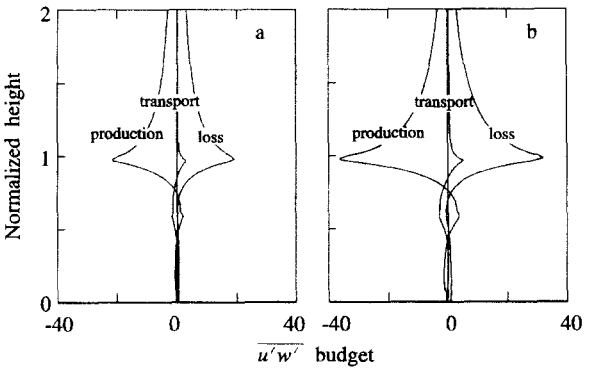

Fig. 5. Budget of the longitudinal Reynolds stress for the deciduous forest calculated using the second-order closure model with 0 (a) and 3 hPa (100 km)$^{-1}$ (b) for the surface pressure gradient. All three terms are nondimensionalized by u_{*2}^3/h.

above, the structure is similar to the numerical (Wilson and Shaw, 1977; Meyers and Baldocchi, 1991; Meyers and Paw U, 1987) and experimental results (Raupach et al., 1986; Meyers and Baldocchi, 1991) obtained for various vegetation stands. The results presented here differ in two respects from the observations and the numerical calculations made for the same forest by Meyers and Baldocchi (1991). A slightly positive production term is created here in the layer below the crown where the vertical velocity gradient is negative, while Meyers and Baldocchi showed that the budget terms were not discernible below $z/h = 0.7$. Their modelled results for the layer $z/h > 0.8$, based on higher-order closure principles, agreed well with the observations. In contrast, the magnitudes near the tree-tops presented in Fig. 5 are smaller than their observed values.

4. Conclusions

Calculations based on first- and second-order closure models show that the mean wind speed within forests can have a strong dependence on the mean horizontal pressure gradient. The inclusion of the pressure gradient terms in the momentum equations allows the FOC model with a simple mixing length parameterization to reproduce secondary wind speed maxima in the trunk space of forests and can improve the predictive ability of the SOC model for flow in forests. The calculations also suggest that significant wind direction shear can occur within forests. The Reynolds stress profile, on the other hand, is less sensitive to the pressure gradient.

There is a possibility that the improvement shown here is fortuitous because no direct measurements of the pressure gradient were available to allow rigorous evaluation of the modelled results. Further experimental validation of the models is therefore needed.

Because the FOC model ignores the non-local effects, the calculated profiles of wind speed and direction are very sensitive to the mean pressure gradient. This is believed to be unrealistic. Models based on more advanced closure schemes have been

developed (e.g. Meyers and Paw U, 1986; Wilson, 1988), in which the physics of canopy turbulence is better described. It remains to be seen how the mean flow simulated with these models responds to the mean pressure gradient.

Acknowledgement

We acknowledge helpful discussions on this work with D.D. Baldocchi, D.C. Steyn, M. D. Novak and X. Cai. We are also grateful to K. T. Paw U and the two reviewers for their constructive criticisms.

References

Baldocchi, D.D. and Hutchison, B.A., 1987. Turbulence in an almond orchard: vertical variation in turbulence statistics. Boundary-Layer Meteorol., 40: 127–146.

Baldocchi, D.D. and Meyers, T.P., 1988a. Turbulence structure in a deciduous forest. Boundary-Layer Meteorol., 43: 345–364.

Baldocchi, D.D. and Meyers, T.P., 1988b. A spectral and lag-correlation analysis of turbulence in a deciduous forest canopy. Boundary-Layer Meteorol., 45: 31–58.

Cionco, R.M., 1965. A mathematical model for air flow in a vegetative canopy. J. Appl. Meteorol., 4: 517–522.

Eckman, R.M., Dobosy, R.J. and Pendergrass, W.R., 1992. Preliminary analysis of wind data from the Oak Ridge site survey. NOAA Technical Memorandum ERL ARL-193. Air Resources Laboratory, Silver Spring, MD, 45 pp.

Finnigan, J.J., 1979. Turbulence in waving wheat. I: mean statistics and honami. Boundary-Layer Meteorol., 16: 181–211.

Green, S.R., 1993. Modelling turbulent air flow in a stand of widely-spaced trees. PHOENICS J. Comput. Fluid Dyn. Appl. (submitted)

Holland, J.Z., 1989. On pressure-driven wind in deep forests. J. Appl. Meteorol., 28: 1349–1355.

Jackson, P.S. and Hunt, J.C.R., 1975. Turbulence wind flow over a low hill. Q. J. R. Meteorol. Soc., 101: 929–955.

Kondo, J. and Akashi, S., 1976. Numerical studies on the two-dimensional flow in horizontally homogeneous canopy layers. Boundary-Layer Meteorol., 10: 255–272.

Lee, X. and Black, T.A., 1993. Atmospheric turbulence within and above a Douglas-fir stand. Part I: statistical properties of the velocity field. Boundary-Layer Meteorol., 64: 149–174.

Li, Z., Miller, D.R. and Lin, J.D., 1985. A first-order closure scheme to describe counter-gradient momentum transport in plant canopies. Boundary-Layer Meteorol., 33: 77–83.

Li, Z., Lin, J.D. and Miller, D.R., 1990. Air flow over and through a forest edge: a steady-state numerical simulation. Boundary-Layer Meteorol., 51: 179–197.

Meyers, T.P. and Baldocchi, D.D., 1991. The budgets of turbulent kinetic energy and Reynolds stress within and above a deciduous forest. Agric. For. Meteorol., 53: 207–222.

Meyers, T.P. and Paw U, K.T., 1986. Testing of a higher-order closure model for modeling airflow within and above plant canopies. Boundary-Layer Meteorol., 37: 297–311.

Meyers, T.P. and Paw U, K.T., 1987. Modelling the plant canopy micrometeorology with higher-order closure principles. Agric. For. Meteorol., 41: 143–163.

Pinker, R.T. and Holland, Z.J., 1988. Turbulence structure of a tropical forest. Boundary-Layer Meteorol., 43: 43–63.

Raupach, M.R., Coppin, P.A. and Legg, B.J., 1986. Experiments on scalar dispersion within a model plant canopy. Part I: the turbulence structure. Boundary-Layer Meteorol., 35: 21–52.

Shaw, R.H. 1977. Secondary wind speed maxima inside plant canopies. J. Appl. Meteorol., 16: 514–523.

Shaw, R.H. and Schumann, U., 1992. Large-eddy simulation of turbulent flow above and within a forest. Boundary-Layer Meteorol., 61: 47–64.

Shaw, R.H. and Pereira, A.R., 1982. Aerodynamic roughness of a plant canopy: a numerical experiment. Agric. Meteorol., 26: 51–65.

Shaw, R.H. and Zhang, X., 1992. Evidence of pressure-forced turbulent flow in a forest. Boundary-Layer Meteorol., 58: 273–288.

Shaw, R.H., den Hartog, G., King, K.M. and Thurtell, G.W., 1974. Measurements of mean wind flow and three-dimensional turbulence intensity within a mature corn canopy. Agric. Meteorol., 13: 419–425.

Shaw, R.H., Paw U, K.T., Zhang, X.J., Gao, W., den Hartog, G. and Neumann, H.H., 1990. Retrieval of turbulent pressure fluctuations at the ground surface beneath a forest. Boundary-Layer Meteorol., 50: 319–338.

Shinn, J.H., 1971. Steady-state two-dimensional air flow in forest and the disturbance of surface layer flow by a forest wall. R & D Tech. Rep. ECOM-5383, Atmos. Sci. Lab., White Sands Missile Range.

Smith, F.B., Carson, D.J. and Oliver, H.R., 1972. Mean wind-direction shear through a forest canopy. Boundary-Layer Meteorol., 3: 178–190.

Verma, S.B., Baldocchi, D.D., Anderson, D.D., Matt, D.R. and Clement, R.J., 1986. Eddy fluxes of CO_2, water vapour, and sensible heat over a deciduous forest. Boundary-Layer Meteorol., 36: 71–91.

Wallace, J.M. and Hobbs, P.V., 1977. Atmospheric Science: An Introductory Survey. Academic Press, New York, 467 pp.

Wilson, J.D., 1988. A second-order closure model for flow through vegetation. Boundary-Layer Meteorol., 42: 371–391.

Wilson, N.R. and Shaw, R.H., 1977. A higher order closure model for canopy flow. J. Appl. Meteorol., 14: 1197–1205.

Yamada, T., 1982. A numerical model study of turbulent airflow in and above a forest canopy. J. Meteorol. Soc. Japan. 60: 439–454.